## SUPPLEMENTAL METHODS

**MHCII/CD11c and MHCII/F4/80 immunostaining and image processing.** Tissues were fixed overnight at 4˚ C in 4% paraformaldehyde, equilibrated in 30% sucrose, then embedded in OCT compound (Tissue Tek, Torrance, CA). Serial sections, cut at 5 μm, were post-fixed in acetone for 5 min, air-dried for 30 min, then treated with 3% $H_2O_2$/0.1% sodium azide in PBS for 30 min. After blocking in 1% BSA/3% donkey serum/0.1 mg/ml hamster IgG for 1 h. FITC-conjugated anti-MHCII (2G9; BD Biosciences), diluted 1/100 in 1% BSA, was applied for 1 h at room temperature along with either biotinylated anti-CD11c (clone HL3; BD Biosciences) or biotinylated anti-F4/80 (C1:A3-1; Cedarlane Laboratories, Burlington, NC) diluted 1/100 or 1/200, respectively. Horseradish peroxidase (HRP)-conjugated streptavidin (Jackson Immunoresearch, West Grove, PA) was then applied at a 1/20,000 dilution in TNB buffer (Perkin Elmer, Wellesley, MA), followed by biotin-tyramide amplification (Perkin Elmer) and incubation with streptavidin-Alexa 594 (Invitrogen). The sections were then retreated with 3% $H_2O_2$/0.1% sodium azide in PBS for 30 min, reblocked with 1% BSA/3% donkey serum containing a streptavidin blocking reagent (Vector Laboratories, Burlingame, CA), and then incubated with HRP-conjugated rabbit anti-FITC antibodies (Invitrogen) diluted 1/200 in TNB buffer plus a biotin blocking reagent (Vector Laboratories) for 30 min at room temperature. The sections were then subjected to further biotin-tyramide amplification, and lastly incubated with streptavidin-Alexa 488 (Invitrogen). All washes were in PBS, and sections were counterstained with DAPI (Sigma). Rigorous controls involving the entire staining protocol but using each primary antibody separately insured that each signal was specific for the intended antigen.

Microscopy was performed using a Zeiss AxioImager M1 (Carl Zeiss MicroImaging, Thornwood, NY) fitted with a motorized stage for automated image collection and an AxioCam MRm digital camera. 10X images collected with FITC, Texas red, and DAPI filter sets were tiled together using AxioVision software (Carl Zeiss MicroImaging). To create panoramic views of implantation sties that would also reveal the location of potential DCs, the images were first manipulated using the Curves command in Adobe Photoshop (Adobe Systems, San Jose, CA) to enhance brightness and contrast. High intensity pixels were then dilated using the Maximum filter of Image J software (1) prior to further enhancement of brightness and contrast using the Window/Level command. Each manipulation was applied equally over an entire image,

however the degree of a given manipulation varied between images in order to compensate for the natural variation in final staining intensity between different samples. Some of the images presented in Figure 5 are shown in close-up in Supplemental Figure S5 before and after their manipulation in Image J. To clearly visualize $MHCII^+$ $CD11c^+$ double positive cells, the green (MHCII) and red (CD11c) green channels were merged using the 'AND' gate function in the Image Calculator of Image J.

**Determination of tissue densities.** Leukocyte tissue densities in the uterus were determined either by flow cytometry or by histomorphometry. The flow cytometric approach was based upon weighing dissected tissues prior to their enzymatic dispersal. Total viable cell numbers were then determined using a hemocytometer with trypan blue exclusion, allowing calculation of total viable cells per mg tissue. Multiplying this value with the percent representation of a cell subset of interest, as determined by flow cytometry, allowed calculation of that subset's density in the units of cells/mg tissue. The histomorphometric approach was based upon staining frozen tissue sections as above with antibodies towards MHCII and F4/80. DCs were defined as $DAPI^+$ $MHCII^+$ $F4/80^-$ entities using the Image Calculator function of Image J and enumerated within the endometrium and myometrium using Analyze Particle function for particle size greater than 2 μm. This analysis gave data in the units of cells/$mm^2$ cross-sectional area. Data for an individual mouse was averaged from 2-4 separate sections.

The flow cytometric approach could be directly applied to determine tissue layer-specific leukocyte densities (in cells/mg tissue) on E7.5, E10.5, and E12.5 since the myometrium could be cleanly dissected from the decidua on these days of gestation. To determine leukocyte densities in the same units in the virgin myometrium and endometrium and the E4.5 myometrium and nascent decidua, where the tissue layers could not be easily separated, we took advantage of our histomorphometric analysis showing that DCs were equally dense within the virgin myometrium and endometrium (Figure 1C-E). Thus, DC tissue densities in whole virgin uteri and whole E4.5 implantation sites, as determined by flow cytometry, could be taken to closely reflect the DC tissue densities of their respective tissue layers. Furthermore, since the endometrium comprised 49.3% +/- 1.3% (mean +/- S.D.) of the cross-sectional area of the progesterone-treated virgin uterus, we could estimate DCs in E4.5 implantation sites to be equally partitioned, in absolute number, between the nascent decidua and the myometrium.

These values, as shown in Figure 4B, were thus calculated simply as the cell number per entire implantation site divided by two. Since histomorphometry revealed that endometrial and myometrial tissue densities of F4/80$^+$ cells were also equivalent (data not shown), it was reasonable to assume that other myeloid cell types would show similar partitioning in the virgin and E4.5 uterus.

**CFSE, LYVE-1, CCL21, and PROX1 immunostaining.** For CFSE, LYVE-1 and CCL21 immunostaining, tissues were fixed in paraformaldehyde, embedded in paraffin, and sectioned at 5 μm. For PROX-1 immunostaining, frozen sections were prepared as above. The subsequent staining protocol was the same as above, simplified for use with only one primary antibody. Paraffin sections were also trypsinized as previously described (2). Rabbit anti-LYVE-1 and rabbit anti-PROX1 antibodies were purchased from AngioBio (Del Mar, CA), and goat anti-CCL21 antibodies were purchased from R&D Systems (Minneapolis, MN). CFSE was detected using HRP-conjugated anti-FITC antibodies (Invitrogen).

**Quantitative RT-PCR.** Total RNA was isolated with Trizol (Invitrogen), and cDNA was prepared from 1 μg of RNA with the iScript cDNA synthesis kit (BioRad, Hercules, CA). Quantitative RT-PCR was performed on 5-10 ng of cDNA using an iCycler thermocycler (BioRad) as previously described (3) and using the nucleic acid dye EvaGreen (Biotium, Hayward, CA) at 1X concentration. Transcript expression levels were normalized to β-actin using $\Delta C_T$ values, with error bars extrapolated from the S.D. of the $\Delta C_T$ mean for each group. We used the following primers purchased from Sigma-Genosys (listed 5' to 3' in the order of forward primer, reverse primer): *β-actin*, GCTCTGGCTCCTAGCACCAT, GCCACCGATCCACACAGAGT; *Ccl21,* ACCAAGTTTAGGCTGTCCCATC, CACATAGCTCAGGCTTAGAGTGCT; *Ccl19,* GTGCCTGCTGTTGTGTTCA, GAGGCCTGGTCCTCTCTTCT; *Cxcl12,* GCTCTGCATCAGTGACGGTAA, AATTTCGGGTCAATGCACAC; *Ccl1,* CTGCTGCTTGAACACCTTGAAG, CTCCTGACTACCACAGCTGGG; *Ccl2*, GGCTGGAGAGCTACAAGAGGATC, CTCTTGAGCTTGGTGACAAAAACTAC; *Ccl5,* CATATGGCTCGGACACCACT, ACACACTTGGCGGTTCCTTC; *Ccl7,* TCCCCAAGAGGAATCTCAAGAG, TTTGTCTTGAAGATAACAGCTTCCC; *Ccl8*, CCCTTCGGGTGCTGAAAAG,

TGGTCTGGAAAACCACAGCTT; *Ccl9,* GCCGGGCATCATCTTTATCA, CGTGGTTGTGAGTTTTGCTCC; *Ccl20*, AAAATCTGTGTGCGCTGATCC, TCTTCTTGACTCTTAGGCT.

**SUPPLEMENTAL REFERENCES**


1. Abramoff, M.D., Magelhaes, P.J., and Ram, S.J. 2004. Image processing with Image J. *Biophotonics International* 11:36-42.
2. Erlebacher, A., Vencato, D., Price, K.A., Zhang, D., and Glimcher, L.H. 2007. Constraints in antigen presentation severely restrict T cell recognition of the allogeneic fetus. *J Clin Invest* 117:1399-1411.
3. Wang, Y., Zhu, W., and Levy, D.E. 2006. Nuclear and cytoplasmic mRNA quantification by SYBR green based real-time RT-PCR. *Methods* 39:356-362.

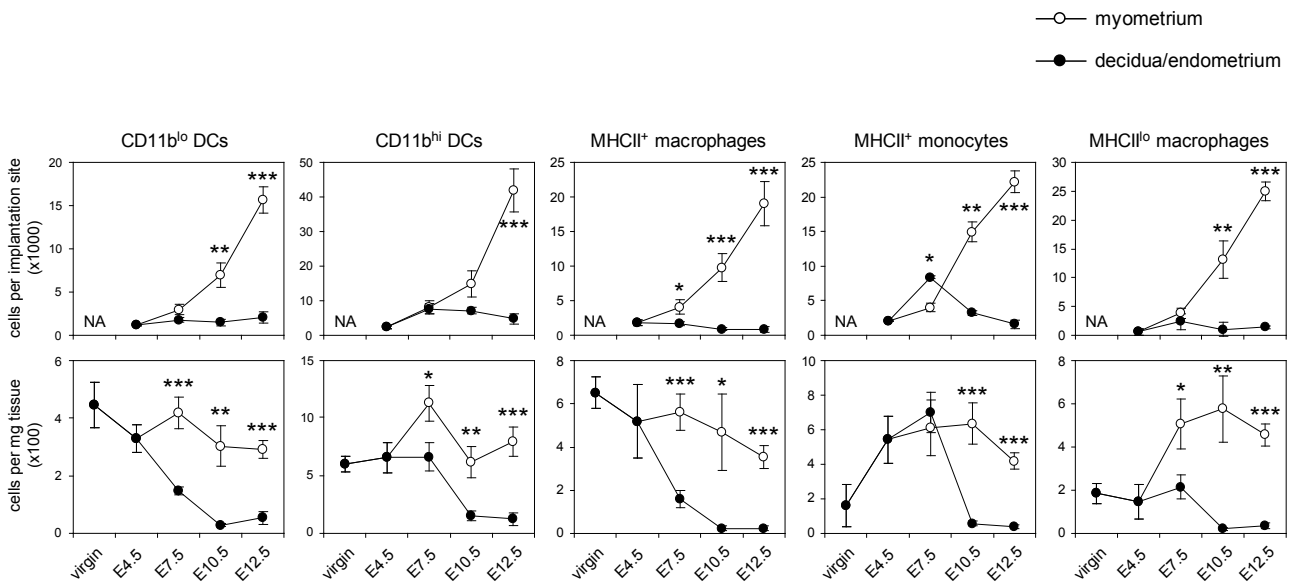


Supplemental Figure S1. Quantification of absolute cell numbers per implantation site and cell number per mg tissue (i.e. tissue density) for additional cell populations visible in Figure 4: $CD11b^{lo}$ DCs (gate v); $CD11b^{hi}$ DCs (gate vi); $MHCII^{+}$ macrophages (gate iii); $MHCII^{+}$ monocytes (gate iv); and $MHCII^{lo}$ macrophages (gate vii). Tissue densities for the myometrium and endometrium of virgin uteri, and for the myometrium and nascent decidua on E4.5 were calculated from raw data as described in the Methods section. Data show mean +/- S.E.M. for *n*=4-7 mice per group. *, $P<0.05$; **, $P<0.02$; ***, $P<0.005$ versus decidua. NA, not applicable.

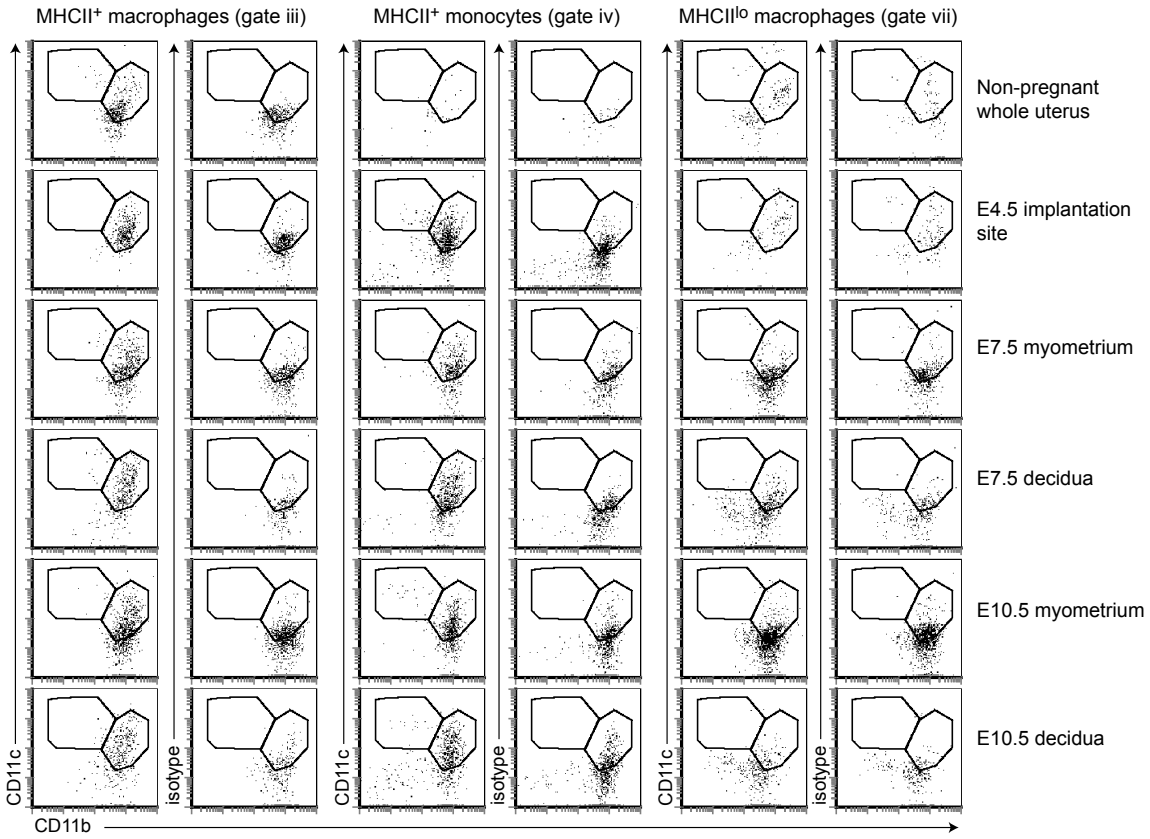


Supplemental Figure S2. CD11b and CD11c expression profiles of various myeloid populations in the non-pregnant and pregnant uterus. Cell suspensions were analyzed by flow cytometry and gated as described in Figure 4. The two gates shown here are the same $CD11b^{lo}$ and $CD11b^{hi}$ DC gates shown in Figure 4.

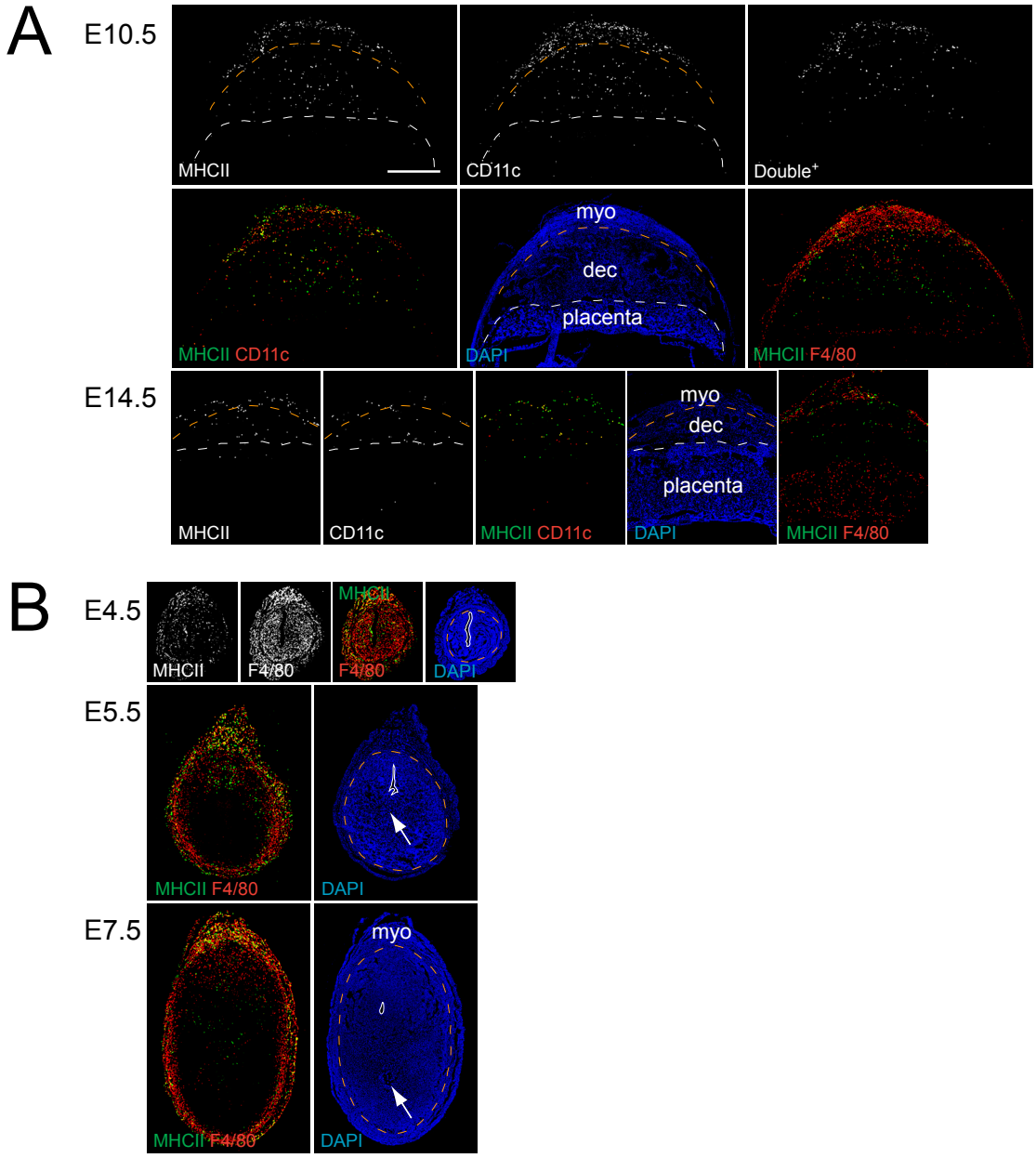


Supplemental Figure S3. Additional immunohistochemical analysis of DC and macrophage distributions in the pregnant uterus. (A) DC and macrophage distributions in the E10.5 and E14.5 pregnant uterus. Adjacent transverse sections, with their mesometrial poles oriented upwards, were double stained with antibodies to MHCII (green) and CD11c (red) or MHCII (green) and F4/80 (red), as indicated, and counterstained with DAPI. Single channel images and combined MHCII/CD11c images after their 'AND' gating (Double$^+$ cells) are shown in black and white. Orange dashed lines demarcate the decidua (dec) from the myometrium (myo), and white dashed lines demarcate the placenta from the decidua. The sections show only the placenta, mesometrial decidua, and the mesometrial half of the myometrium; the embryo is located below each panel. (B) Macrophage distributions in the E4.5, E5.5 and E7.5 pregnant uterus. The DAPI-stained sections are the same images, with annotations, as those shown in Figure 5. The other images are from adjacent sections stained with antibodies to MHCII (green) and F4/80 (red). Single channel images are shown in black and white. To visualize DCs and macrophages in panoramic view, the images were manipulated as described in the Methods section; some are shown at higher magnification in Supplemental Figure S4. The scale bar (1 mm) applies to the entire figure.

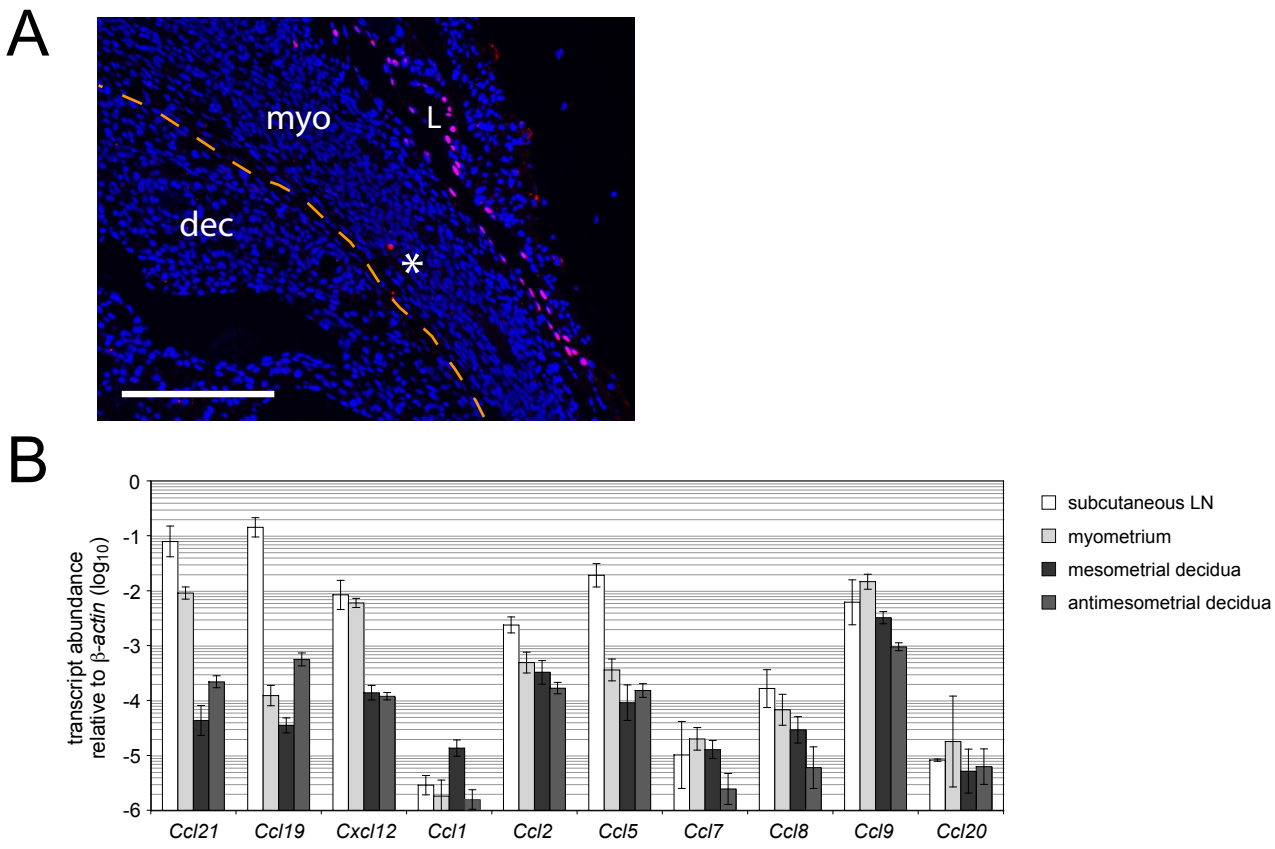


Supplemental Figure S4. (A) PROX-1 immunostaining (red) of an E10.5 implantation site with DAPI counterstain (blue). The orange dashed line demarcates the decidua (dec) from the myometrium (myo); L indicates a lymphatic vessel. The image is from the mesometrial side of the implantation site. Punctate background staining (*) was not nuclear associated. Scale bar=100µm. (B) Chemokine mRNA expression level in the pregnant uterus. Implantation sites were harvested on E8.5 of pregnancy, the myometrium was separated from the decidua, and the decidua was bisected into mesometrial and antimesometrial sections with the embryonic tissue removed. Data show mean transcript abundance compared to β-*actin* +/- S.D. of 2 mice for the lymph nodes and 3 mice for the uterine tissue samples each with two pooled implantation sites.

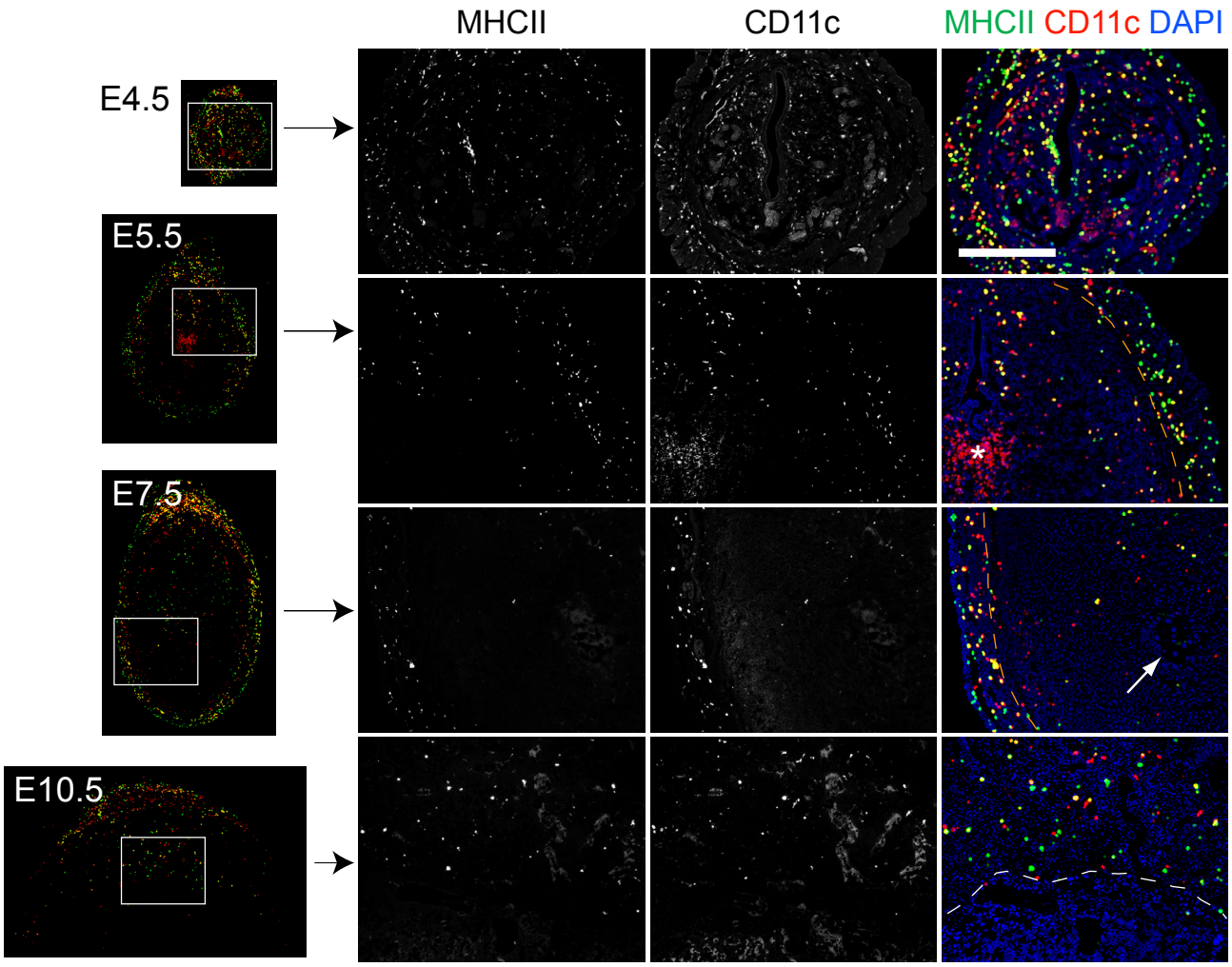


Supplemental Figure S5. Validation of the image enhancements described in the Methods section. The MHCII (green) /CD11c (red) double immunostained images on the left side of the figure are the same ones shown in Figure 5 and Supplemental Figure S3. The right set of panels show higher magnifications of the boxed areas. The black and white images show individual MHCII and CD11c channels after nonlinear adjustment in Adobe Photoshop, but prior to their further manipulation with Image J software. The high magnification color images, with DAPI counterstain, are the merged images after Image J manipulation to dilate the cells and hence render them visible in a panoramic view. The asterisk shows an area of non-specific staining also seen in the absence of primary antibody; the arrow indicates a group of trophoblast giant cells lateral to an implanted embryo. Orange dashed lines demarcate the decidua from the myometrium, and the white dashed line demarcates the placenta from the decidua. Scale bar=0.5 mm.